Large-disturbance Stability Analysis of DC Microgrid with Constant Power Load and Its Transient Voltage Stability Control Strategy

Li Zekun[1,2] Pei Wei[1,2] Kong Li[1,2]
1. Institute of Electrical Engineering, Chinese Academy of Sciences, Beijing, China
2. University of Chinese Academy of Sciences, Beijing, China

***Abstract*—As the important part of future AC/DC hybrid distribution networks, maintaining the voltage stability of DC microgrid is very important for the safe operation of the distribution network. Based on Brayton-Moser's mixed potential theory, this paper first studies the large disturbance stability of a DC microgrid with constant power load. Then, the stability criterion of the analytic form of the system under large disturbance is obtained, which the effects of parameters such as AC side inductance, resistance, controller control parameters, and constant power load power values on the system stability are taken into account. According to the criterion, a stability control strategy for energy storage system is proposed. This strategy can avoid the unnecessary switching between the master and slave source, ensure the system stable under large disturbances and help the system quickly return to the stable state. The criterion and stability control strategy are simple and can be easily implemented. Simulation results demonstrate that the stability criterion and the control strategy are effective.**

***Index Terms*—voltage source converter; large-disturbance stability analysis; mixed potential theory; control strategy**

I. INTRODUCTION

THE increasing capacity of the modern power electronic loads and distributed generations in distribution network promotes DC microgrid become one of the main power supply structures for future communities, buildings and homes [1].

In the grid-connected mode, the DC microgrid is connected to AC grid through the voltage source converter(VSC). For the full use of renewable energy, the renewable energy generations are usually operated in MPPT mode [2]. To reduce the number of cycles of the energy storage and increase the service life, the state of energy storage should be determined according to the state of charge. In the above situation, the renewable energy and the energy storage cannot be used as the DC bus voltage controller. For DC microgrid with only single grid-connected VSC, master-slave control is a good choice, and the DC bus voltage can be controlled by VSC to facilitate the bidirectional energy flow between the AC and DC grids. Most loads in DC microgrid are connected to DC bus through tight controlled converters, which can be equivalent to constant power loads(CPLs) with negative impedance characteristics [1].

In large disturbances, the nonlinearity of power electronics in DC microgrid may cause the system to crash, and an appropriate control strategy is needed. Thus, to guide the development of control strategies, it is also necessary to analyze the system's large signal stability and quantitatively explore the influence of system parameters and control parameters on stability.

Large-disturbance stability analysis of DC microgrid requires analysis method based on nonlinear system theory. Brayton-Moser's mixed potential theory is an effective tool for large-signal stability analysis of nonlinear systems and can derive analytic large-signal stability criterion of nonlinear system [3].

In [4], this theory is applied to analyze the attraction domain of a DC system with parallel CPLs, but the obtained stability criterion requires a high filter capacitance. In [5], the criterion of a DC system with multistage LC filter under large disturbance is obtained by mixed potential theory, however, the situation when the DC power source is the source converter is not considered. In [6], the large disturbance stability of 18-pulse rectifier DC system is analyzed, but the influence of control parameters is not considered. Literature [3] and [7] quantitatively analyzes the influence of controller parameters on the stability of BUCK/BOOST converter with CPL using the theory. However, the large-signal stability analysis of DC microgrid with VSC is rarely involved.

For consideration of cost and fast response, a fast voltage coordinated control strategy without communication in large disturbances is needed [8]. In [9,10], various DC microgrid coordination control strategies based on DC bus signals(DBS)

This work is supported by The National Key Research and Development Program of China (2017YFB0903300).

Li Zekun is with the Institute of Electrical Engineering, Chinese Academy of Sciences and University of Chinese Academy of Sciences (e-mail: lizekun@mail.iee.ac.cn).

have been proposed. In the above strategy, the system will switch the work mode of converters according to DBS to maintain the system stability during large disturbances.

Actually, the energy storage can compensate the DC bus to help maintain system stability and avoid the adverse effects on stability caused by frequent control mode switching due to the disordered fluctuation of renewable power generation and load.

In this paper, based on mixed potential theory, the large signal stability criterion of a DC microgrid which the VSC is the voltage controlled master source is studied. And according to the criterion, a transient control strategy for energy storage system is proposed. With this strategy, in the condition that the load power does not exceed the rated power of the system, the energy storage can help maintain large-disturbance stability and avoid frequent control mode switching.

II. Structure and Mathematical Model of DC Microgrid

A. Structure of DC Microgrid

In this paper, the DC microgrid is working in grid-connected mode and consists of the following parts: 1) The AC side of VSC is three-phase symmetrical, and VSC is the master converter; 2) Photovoltaic generation unit is working at MPPT mode and can be regarded as a negative power CPL. And the tightly controlled power electronic load can also be equivalent to a CPL. 3) Because the cables are short, the DC bus's impedance is ignored. 4) The energy storage is operated at current controlled mode, and injects current into the DC bus or absorbs current from the DC bus according to DBS.

The topology of the DC microgrid is shown in Fig.1.

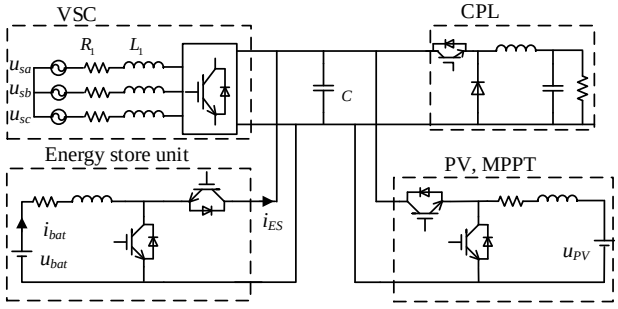

Fig.1 Topology of DC microgrid

B. Mathematical Model of DC microgrid

The state equation of the grid-connected VSC under the *dq* coordinate system is

$$\begin{cases} L_1 \dfrac{di_{sd}}{dt} = u_{sd} - R_1 i_{sd} + \omega L_1 i_{sq} - v_d \\ L_1 \dfrac{di_{sq}}{dt} = u_{sq} - R_i i_{sq} + \omega L_1 i_{sd} - v_q \end{cases} \tag{1}$$

where L_1 and R_1 are the equivalent connection reactance and resistance of the AC side of VSC; ω is the angular frequency of the AC system; u_{sd} and u_{sq} are the component of the AC grid voltage on the *d*-axis and *q*-axis; i_{sd} and i_{sq} are the *d*-axis current and *q*-axis current; v_d and v_q are the component of the voltage of the VSC's AC side on the *dq* axis.

The grid-connected VSC usually adopts double closed-loop control. For the current inner loop, PI control is used in this paper. When the PI parameters are set properly, the inner loop can be regarded as a first-order inertia link, and if the time constant of the current loop is set to 15-20 times the sampling period, the current loop can be further equivalent to 1[11]. That is to say, it can be approximated that the current loop can track the reference value of the outer loop output without delay.

The VSC voltage outer loop adopts constant DC voltage control and constant reactive power control. In this paper, the VSC is operated in the unit power factor state, which means i_{sq} is set to 0 and the *q*-axis of VSC does not transmit power to the DC side. Based on the above analysis, there is

$$i_{sd} = i_{sdref} = k_{vp}(u_{dcref} - u_{dc}) + k_{vi}\int (u_{dcref} - u_{dc})dt \tag{2}$$

where k_{vp} and k_{vi} are proportional and integral parameters of voltage loop; u_{dc} and u_{dcref} are the DC bus voltage and its reference value. The DC side output current of VSC is

$$i_o = \frac{3}{4}(m_d i_{sd} + m_q i_{sq}) = \frac{3}{2}\frac{v_d i_{sd}}{u_{dcref}} \tag{3}$$

where m_d and m_q are the modulation ratios.

Since the line impedance is not considered, the photovoltaic unit and load can be equivalent to a CPL. When the energy storage is blocked, the state equation of DC bus voltage is

$$\begin{cases} C\dfrac{du_{dc}}{dt} = i_o + i_{ES} - i_{CPL} \\ i_{CPL} = P_{CPL}/u_{dc} \end{cases} \tag{4}$$

where, i_{CPL} and P_{CPL} are the current and power of equivalent CPL; i_{ES} is the output current of energy storage. If the power is injected into the bus, i_{ES} is positive, otherwise it is negative.

III. Derivation of Large-Disturbance Stability Criterion Based on Mixed Potential Theory

A. Introduction of mixed potential theory

Mixed potential function is a special form of Lyapunov function, and literature [12] first proposed the application of mixed potential function in nonlinear circuits. Mixed potential function has the following standard form,

$$P(i,v) = -A(i) + B(v) + (i, \gamma v - \alpha) \tag{5}$$

where -A(i) is current potential and B(v) is voltage potential; i is the current through the inductors, and v is the voltage on the capacitor; γ and α are constant vectors.

The third stability theorem of mixed potential theory used in

this paper is given as below.

μ_1 is the minimum eigenvalue of $L^{-1/2}A_{ii}(i)\,L^{-1/2}$, and μ_2 is the minimum eigenvalue of $C^{-1/2}B_{vv}(v)\,C^{-1/2}$, where $A_{ii}(i)=\partial^2 A(i)/\partial i^2$, $B_{vv}(v)=\partial^2 B(v)/\partial v^2$. If for any i and v in the system, there is

$$\mu_1+\mu_2>0$$

and when $|i|+|v|\to\infty$, there is

$$(\frac{\mu_1-\mu_2}{2})P(i,v)+\frac{1}{2}(P_i,L^{-1}P_i)+\frac{1}{2}(P_v,C^{-1}P_v)\to\infty$$

where $A_i(i)=\partial A(i)/\partial i$, $B_v(v)=\partial B(v)/\partial v$. And then the system will finally approach the equilibrium point.

B. Derivation of the system's large-disturbance criterion

According to the analysis in the previous section, for the DC side of the microgrid, VSC can be equivalent to a controlled current source which the current is i_o in formula (3). Energy storage can be equivalent to a controlled current source i_{ES}; photovoltaic unit and load can be equivalent to a CPL. The simplified model of the system is shown in Figure 2.

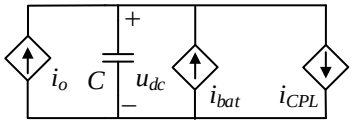

Fig.2 Simplified model of the system

For the circuit of Fig.2, the current potential function is

$$\int_\Gamma\sum_\mu v_\mu di_\mu=\int_\Gamma u_{dc}di_o+\int_\Gamma u_{dc}di_{ES}-\int_\Gamma u_{dc}di_{CPL}$$

$$=i_o\cdot u_{dc}-\int_0^{u_{dc}}i_o dv+i_{ES}\cdot u_{dc}- \tag{6}$$

$$\int_0^{u_{dc}}i_{ES}dv-P_{CPL}+\int_0^{u_{dc}}\frac{P_{CPL}}{v}dv$$

The voltage-current product of the capacitor branch is

$$\sum_\sigma i_\sigma v_\sigma\,|_\Gamma=-(i_o+i_{ES}-\frac{P_{CPL}}{u_{dc}})\cdot u_{dc} \tag{7}$$

System's mixed potential function is the sum of (6) and (7),

$$P(i,v)=-\int_0^{u_{dc}}i_o dv-\int_0^{u_{dc}}i_{ES}dv+\int_0^{u_{dc}}\frac{P_{CPL}}{v}dv \tag{8}$$

System's mixed potential function (8) can be rewritten as the standard form in (5) as follows,

$$\begin{cases}A(i)=0,(i,\gamma v-\alpha)=0\\ B(v)=-\int_0^{u_{dc}}i_o dv-\int_0^{u_{dc}}i_{ES}dv+\int_0^{u_{dc}}\frac{P_{CPL}}{v}dv\end{cases} \tag{9}$$

Based on the third stability theorem, the large-disturbance stability criterion of the system shown in Fig.2 is

$$\begin{cases}\mu_1=\frac{1}{\sqrt{L}}A_{ii}(i)\frac{1}{\sqrt{L}}=0\\ \mu_2=\frac{1}{\sqrt{C}}B_{vv}(v)\frac{1}{\sqrt{C}}=\frac{1}{C}(\frac{-\partial i_o}{\partial u_{dc}}+\frac{-\partial i_{ES}}{\partial u_{dc}}-\frac{P_{CPL}}{u_{dc}^2})\\ \mu_1+\mu_2>0\end{cases} \tag{10}$$

according to formula (2) and formula (3), there is

$$-\frac{\partial i_o}{\partial u_{dc}}=-\frac{3}{2}\frac{\partial v_d i_{sd}/u_{dcref}}{\partial u_{dc}}=\frac{3}{2}\frac{(u_{sd}-2R_1i_{sd})k_{vp}-L_1k_{vi}i_{sd}}{u_{dcref}} \tag{11}$$

combined with equations (10) and (11), there is

$$\frac{3}{2}\frac{(u_{sd}-2R_1i_{sd})k_{vp}-L_1k_{vi}i_{sd}}{u_{dcref}}+\frac{-\partial i_{ES}}{\partial u_{dc}}-\frac{P_{CPL}}{u_{dc}^2}>0 \tag{12}$$

Thus, the inequality (12) is the large-disturbance stability criterion of the system shown in Fig.2.

IV. SYSTEM STABILITY CRITERION ANALYSIS AND SIMULATION VERIFICATION

Firstly, the effectiveness of the criterion inequality (12) is analyzed when the energy storage does not participate in the bus voltage control, however, this doesn't affect the accuracy of the conclusion, and can also provide a theoretical basis for transient control strategy.

In order to analyze the influence of parameters on stability and verify the validity of the stability criterion, firstly, the parameters of the DC microgrid shown in Fig. 1 are given in Table I, and a detailed electromagnetic transient simulation model is built in Simulink.

TABLE I
PARAMETERS OF THE DC MICROGRID

Parameter	Value	Parameter	Value
u_s	190V	u_{dcref}	500V
f	50Hz	f_s	10kHz
k_{ip}	25	k_{ii}	200
C	1.5mF	u_{buck}	150V

In Table I, u_s is AC source line voltage, f is the frequency of the AC system, f_s is the switching frequency of VSC, k_{ip} and k_{ii} are current loop proportional and integral parameters, u_{buck} is the load converter output voltage. Other parameters of the system will be given later.

Formula (12) shows that the parameters which affect the system's large-disturbance stability are VSC's AC side inductance L_1, AC side resistance R_1, VSC voltage outer loop control parameters k_{vp}, k_{vi}, load power P_{CPL}, DC bus voltage u_{dc} and so on.

In order to verify the accuracy of the above analysis, let the equivalent CPL power P_{CPL} step up from 5kW to 15kW at 0.5s. The corresponding simulation results are shown in Fig.3.

TABLE II
PREDICTION OF STABILITY WHEN LOAD POWER SUDDENLY INCREASING

	k_{vp}	k_{vi}	L_1	R_1	criterion
1	0.35	100	4e-3	0.3	Not Satisfying
2	0.46	100	4e-3	0.3	Satisfying
3	0.35	50	4e-3	0.3	Satisfying
4	0.35	100	2e-3	0.3	Satisfying
5	0.35	100	4e-3	0.15	Satisfying

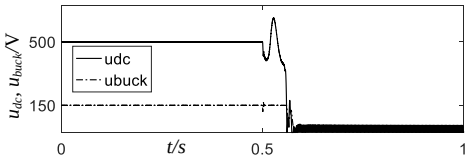

(a) Simulation results of first group of parameters in Table II

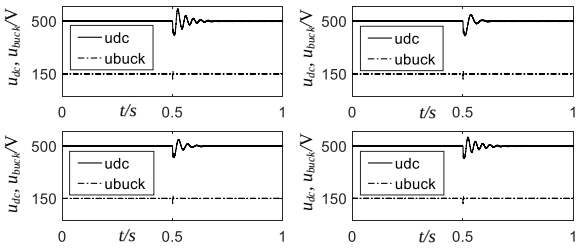

(b) Simulation results of other group of parameters in Table II

Fig.3 Simulation results corresponding to Table II

In Fig.3(a), the system parameters do not satisfy formula (12), and the system cannot maintain stability after large disturbance, both DC bus voltage and load converter voltage drop to zero.

In Fig.3(b), the parameters are modified according to formula (12) to make the system meet the stability criterion. It can be seen from the figure that the DC bus voltage oscillates at 0.5s and after a period of adjustment, the bus voltage finally stabilizes at the set value. At 0.5 s, the output voltage of load converter also has a disturbance. However, the adjustment time is relatively short and negligible, so it can be considered that it maintains the CPL characteristics during the transient process.

According to the calculation results in Table II and the simulation results in Fig.3, it can be seen that the conclusion of the large-disturbance stability analysis is consistent with the simulation results, which can prove the correctness of the stability criterion shown in formula (12).

V. Transient Voltage Stability Control Strategy of Energy Storage and Simulation Verification

A. Control Strategy

The above analysis is performed when the energy storage does not participate in bus voltage control. As can be seen from the above analysis and criterion (12), if the output current of the energy storage satisfies $-\partial i_{ES}/\partial u_{dc} > 0$, the stability of the system can be improved, so that the system can withstand greater disturbance.

According to the criterion (12), there is

$$\frac{-\partial i_{ES}}{\partial u_{dc}} > \frac{P_{CPL}}{u_{dc}^2} - \frac{3}{2}\frac{(u_{sd}-2R_1 i_{sd})k_{vp} - L_1 k_{vi} i_{sd}}{u_{dcref}} \tag{13}$$

Formula (13) is the energy storage compensation control strategy and theoretical basis proposed in this paper. This strategy controls the compensation current i_{ES} based on DC bus voltage instantaneous value u_{dc}. With the fall of u_{dc}, i_{ES} rises according to the slope calculated by (13), which can play a good compensation role and ensure the stable operation of system; in the case of u_{dc} rising, i_{ES} should absorb current from DC bus according to (13).

Based on the above analysis, the transient control strategy of the energy storage can be designed as follows:

$$\begin{cases} i_{ES} = k_{p\_ES}(u_{dcref} - u_{dc}) \\ k_{p\_ES} > \dfrac{P_{CPL}}{u_{dc}^2} - \dfrac{3}{2}\dfrac{(u_{sd}-2R_1 i_{sd})k_{vp} - L_1 k_{vi} i_{sd}}{u_{dcref}} \end{cases} \tag{14}$$

i_{ES} is the current that the energy storage feeds into the DC bus. In this paper, the energy storage adopts the BOOST converter, so the actual controlled current is the battery's current i_{bat}. If the loss is not considered, the relationship between i_{bat} and i_{ES} meets $i_{bat}/i_{ES} = u_{dc}/u_{bat}$, where u_{bat} is the voltage of battery. Thus, the current control strategy of the energy storage battery is

$$i_{bat} = k_{p\_bat}(u_{dcref} - u_{dc}), k_{p\_bat} = k_{p\_ES} \cdot u_{dc}/u_{bat} \tag{15}$$

Formula (14) and (15) is the transient voltage compensation control strategy for energy storage. And the control block diagram is shown in Fig.4.

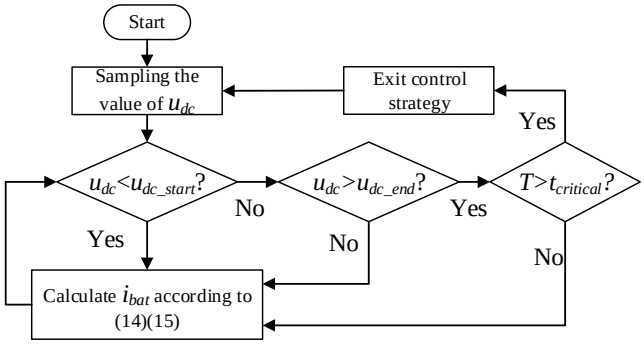

Fig.4 Control block diagram of energy storage

In Fig.4, u_{dc_start} is the voltage when starting the strategy, which is usually 90% to 95% of u_{dcref}. And when u_{dc} is higher than u_{dc_end} and lasts for a while, energy storage exits the control strategy. T is the time which u_{dc} lasts higher than u_{dc_end}, and $t_{critial}$ is critical time. The situation of u_{dc} rising is similar to the case of u_{dc} falling, so it will not be repeated here.

B. Simulation Verification

In order to verify the correctness of the control strategy, the microgrid simulation model shown in Fig.1 is applied in this section. Four sets of system parameters are selected and the stability criteria of their corresponding energy storage current

controller are calculated, which is shown in Table III. The parameters of VSC and energy store are k_{ip}=100, L_1=4mH, R_1=0.3Ω, u_{bat}=200V, and other parameters are shown in Table I. In simulation verification, u_{dc_start} is set to 90% of u_{dcref}, u_{dc_end} is set to 98% of u_{dcref}, and $t_{critial}$ is set to 0.1s. The simulation results are shown in Fig.5

TABLE III
ENERGY STORAGE CURRENT CONTROLLER STABILITY CRITERIA OF DIFFERENT SYSTEM PARAMETERS

	k_{vp}	Initial P_{CPL}	Final P_{CPL}	criterion	k_{p_bat}
1	0.35	5kW	15kW	k_{p_bat}>0.034	0.02
2	0.35	5kW	15kW	k_{p_bat}>0.034	0.04
3	0.46	5kW	17kW	k_{p_bat}>0.031	0.02
4	0.46	5kW	17kW	k_{p_bat}>0.031	0.04

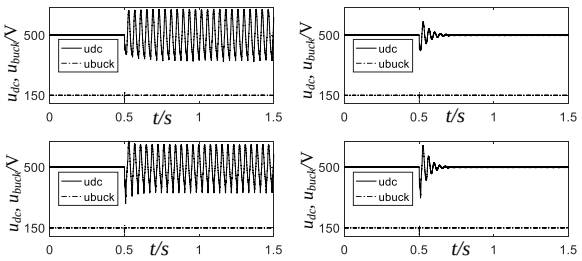

Fig.5 Simulation results corresponding to Table III

The result of the first group's parameters is the upper left part of Fig.5, the result of the second is the upper right part, and so on. As can be seen in Table III and Fig.5, when the energy storage current controller meets the strategy (14) (15), the energy storage can help maintain the system's large disturbance stability, and if not satisfied, it cannot make the system stable under large disturbance. The above results demonstrate the effectiveness of the transient control strategy for energy storage based on large-disturbance stability criteria.

VI. CONCLUSION

This paper analyzes the large-disturbance stability of DC microgrid with grid-connected VSC worked as the master source. The conclusions are as follows:

1) The analytical stability criterion based on mixed potential theory can indicate the influence of system's parameters on the system stability, help provide some guidance for the parameter design during the design process, and reduce the workload of simulation analysis.
2) The transient control strategy of energy storage based on the criterion proposed in this paper can help maintain the system's large-disturbance stability.

In summary, the stability criterion and control strategy of this paper can provide some guidance and help for the stability analysis and integrated operation control of AC/DC hybrid distribution network.

REFERENCES

[1] M. Su, Z. Liu, Y. Sun, H. Han, and X. Hou, "Stability Analysis and Stabilization Methods of DC Microgrid With Multiple Parallel-Connected DC-DC Converters Loaded by CPLs," *IEEE Transactions on Smart Grid,* vol. 9, , pp. 132-142, Jan. 2018.

[2] A. K. Abdelsalam, A. M. Massoud, S. Ahmed, and P. N. Enjeti, "High-Performance Adaptive Perturb and Observe MPPT Technique for Photovoltaic-Based Microgrids," *IEEE Transactions on Power Electronics,* vol. 26, pp. 1010-1021, Apr. 2011.

[3] W. Du, J. Zhang, Y. Zhang, and Z. Qian, "Stability Criterion for Cascaded System With Constant Power Load," *IEEE Transactions on Power Electronics,* vol. 28, pp. 1843-1851, Apr. 2013.

[4] M. Belkhayat, R. Cooley, A. Witulski, "Large signal stability criteria for distributed systems with constant power loads", Proc. IEEE 26th Power Electron. Spec. Conf., pp. 1333-1338, Jun. 1995.

[5] X. Liu, Y. Zhou, W. Zhang, and S. Ma, "Stability Criteria for Constant Power Loads With Multistage LCL Filters," *IEEE Transactions on Vehicular Technology,* vol. 60, pp. 2042-2049, Jun. 2011.

[6] A. Griffo, and J. Wang, "Large Signal Stability Analysis of 'More Electric' Aircraft Power Systems with Constant Power Loads," *IEEE Transactions on Aerospace & Electronic Systems,* vol. 48, pp. 477-489, Jan. 2012.

[7] M. Huang, H. Ji, J. Sun, L. Wei, and X. Zha, "Bifurcation-Based Stability Analysis of Photovoltaic-Battery Hybrid Power System," *IEEE Journal of Emerging and Selected Topics in Power Electronics,* vol. 5, pp. 1055-1067, Sept. 2017.

[8] P. Wang, C. Jin, D. Zhu, Y. Tang, P. C. Loh, and F. H. Choo, "Distributed Control for Autonomous Operation of a Three-Port AC/DC/DS Hybrid Microgrid," *IEEE Transactions on Industrial Electronics,* vol. 62, pp. 1279-1290, Feb. 2015.

[9] F. Nejabatkhah, and Y. W. Li, "Overview of Power Management Strategies of Hybrid AC/DC Microgrid," *IEEE Transactions on Power Electronics,* vol. 30, pp. 7072-7089, Dec. 2015.

[10] Y. Gu, X. Xiang, W. Li, and X. He, "Mode-adaptive decentralized control for renewable DC microgrid with enhanced reliability and flexibility," *IEEE Transactions on Power Electronics,* vol. 29, pp. 5072-5080, Sept. 2014.

[11] V. Blasko, and V. Kaura, "A new mathematical model and control of a three-phase AC-DC voltage source converter," *IEEE Transactions on Power Electronics,* vol. 12, pp. 116-123, Jan. 1997.

[12] R. K. Brayton, and J. K. Moser, "A theory of nonlinear networks. I,II," *Quartery of Applied Math,* vol. 12, pp. 1-33, Apr. 1964.